Int J Earth Sciences (2001) 89 : 793–811
DOI 10.1007/s005310000097

ORIGINAL PAPER

O. Candan · O. Ö. Dora · R. Oberhänsli
M. Çetinkaplan · J. H. Partzsch · F. C. Warkus
S. Dürr

Pan-African high-pressure metamorphism in the Precambrian basement of the Menderes Massif, western Anatolia, Turkey

Received: 17 March 2000 / Revised: 20 March 2000 / Published online: 15 August 2000

Abstract The Menderes Massif is made up of Pan-African basement and a Paleozoic to Early Tertiary cover sequence imbricated by Late Alpine deformation. The Precambrian basement comprises primarily medium- to high-grade schists, paragneisses, migmatites, orthogneisses, metagranites, charnockites, and metagabbros. High-pressure relics in the Pan-African basement are divided into two groups: eclogites and eclogitic metagabbros. The mineral assemblage in the eclogites is omphacite (Jd 44)–garnet–clinozoisite–rutile. The eclogites occur as pods and boudinaged layers in the basement schists and paragneisses. Inclusions found in the cores of the garnets indicate a medium-pressure protolith. The eclogitic metagabbros are closely related to Precambrian gabbroic stocks. The igneous texture and relic magmatic phases are preserved in these high-pressure rocks, which are characterized by the mineral assemblage omphacite (Jd 25)–garnet–rutile±kyanite. The *P–T* conditions of the Pan-African high-pressure metamorphism in the eclogites are estimated to be 644 °C with a minimum pressure of approximately 15 kbar. The eclogites are partly to completely retrograded to garnet amphibolites by a Barrovian-type overprint which developed under isothermal decompression conditions. For this post-eclogitic event, the *P–T* estimates are 7 kbar and 623 °C. The eclogite relics provide strong support for a correlation of the Menderes Massif with the Bitlis Massif in terms of common Pan-African high-pressure evolution.

Keywords Eclogites · Eclogitic metagabbros · Menderes Massif · High-pressure metamorphism

O. Candan (✉) · O. Ö. Dora · M. Çetinkaplan
Dokuz Eylül Universitesi, Mühendislik Fak, Jeoloji Müh, Böl,
35100 Bornova-Izmir, Turkey

R. Oberhänsli · J. H. Partzsch · F. C. Warkus
Institut für Geowissenschaften, Universität Potsdam,
Postfach 601553, 14415 Potsdam, Germany

S. Dürr
Institut für Geowissenschaften,
Johannes Gutenberg Universität Mainz,
55099 Mainz, Germany

Introduction

The Menderes Massif in western Anatolia is structurally bounded to the northwest by the Late Cretaceous Bornova Flysch Zone and to the south by the Mesozoic–Paleogene Lycian nappe complex (Fig. 1). The lithostratigraphic rock succession and new evidence related to the Tertiary high-pressure evolution of the Mesozoic–Early Tertiary sequence of the Menderes Massif provide strong support for a correlation with the Attic-Cycladic crystalline complex in the Aegean Sea (Dürr et al. 1978; Candan et al. 1997; Oberhänsli et al. 1998).

Contrary to previous studies that suggested a simple onion-shaped structural model for the Menderes Massif (Dürr 1975), recent studies have revealed a complex nappe-pile structure that resulted from Late Alpine contractional deformation (Dora et al. 1995; Partzsch et al. 1998; Gessner et al. 1998). The lithostratigraphic succession in this crystalline complex can be divided into two tectono-metamorphic units: a Pan-African basement (core series); and Paleozoic to Early Tertiary metasediments (cover series). The oldest units of the Pan-African basement consist of partially migmatized paragneisses, so-called leptite-gneisses, and medium- to high-grade schists. These Late Proterozoic metasediments were intruded by numerous polymetamorphic Precambrian gabbros and post-metamorphic Pan-African metagranites/orthogneisses (Dora et al. 1995; Hetzel and Reischmann 1996). The Paleozoic–Early Tertiary cover assemblages include Ordovician (?) to Permo-Carboniferous low- to medium-grade phyllites, quartzites, and marbles, Late Tri-

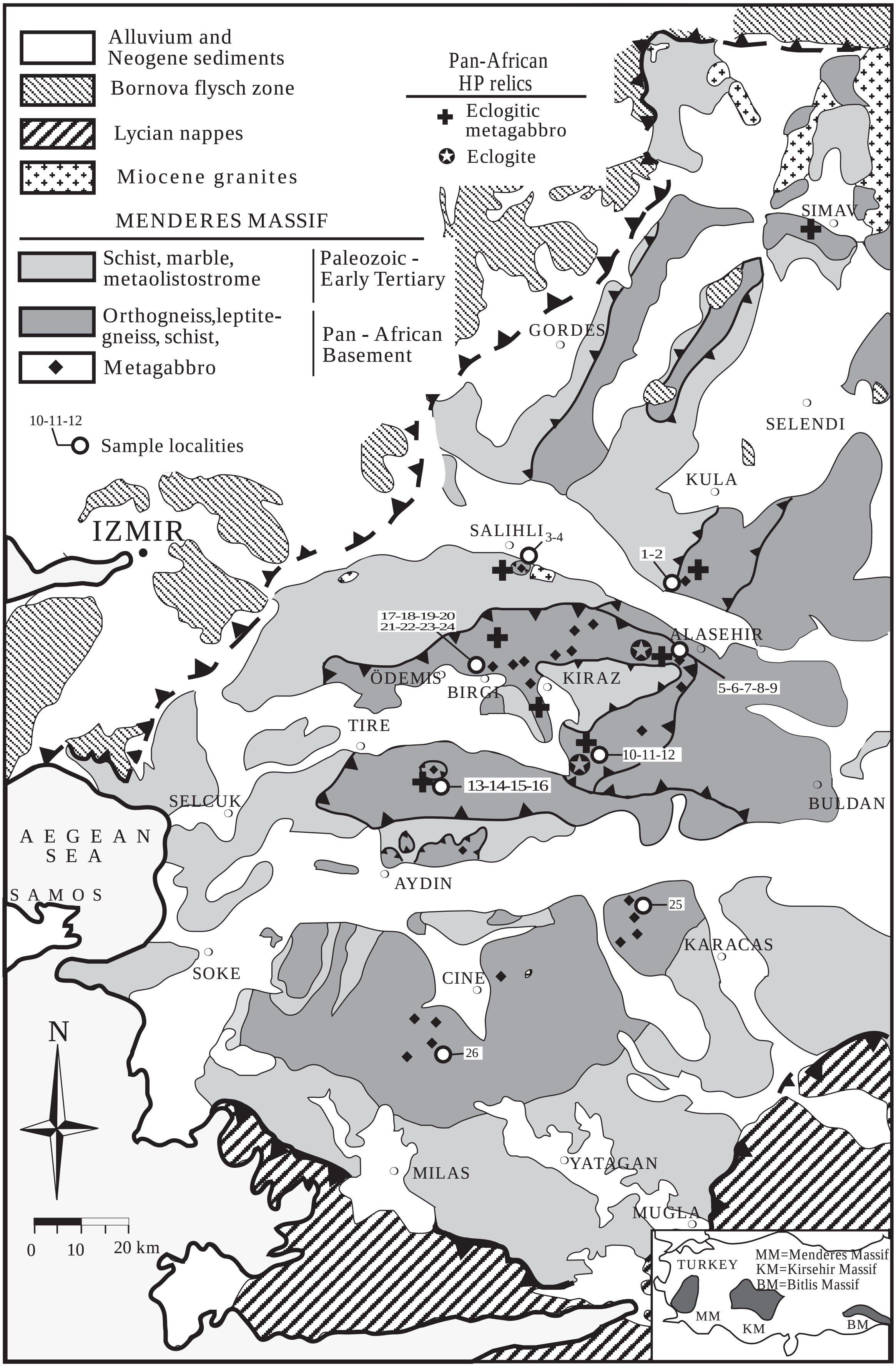

Alluvium and
Neogene sediments
Bornova flysch zone
Lycian nappes
Miocene granites
MENDERES MASSIF
Schist, marble,
metaolistostrome
Paleozoic -
Early Tertiary
Orthogneiss,leptite-
gneiss, schist,
Metagabbro
Pan - African
Basement
10-11-12
Sample localities
Pan-African
HP relics
Eclogitic
metagabbro
Eclogite
IZMIR
GORDES
SIMAV
SELENDI
KULA
SALIHLI
ALASEHIR
ÖDEMIS
BIRGI
KIRAZ
TIRE
SELCUK
BULDAN
AEGEAN
SEA
SAMOS
AYDIN
SOKE
CINE
KARACAS
MILAS
YATAGAN
MUGLA
N
0 10 20 km
3-4
1-2
17-18-19-20
21-22-23-24
5-6-7-8-9
10-11-12
13-14-15-16
25
26
TURKEY
MM=Menderes Massif
KM=Kirsehir Massif
BM=Bitlis Massif
MM
KM
BM

Fig. 1 Generalized geological map of the Menderes Massif and the main localities of Pan-African high-pressure relics (Sample numbers=Kula: *1*=96-128/10, *2*=G-6/A; Salihli: *3*=351/2, *4*=352/2; Alaşehir: *5*=97-241/2, *6*=98-69/4, *7*=98-244, *8*=97-270/13, *9*=98-74/8; Kiraz: *10*=97-184, *11*=97-163, *12*=97-151/7; Tire: *13*=97-120/9, *14*=318/8, *15*=98-73/8, *16*=317/3; Birgi: *17*=98, *18*=96-127/3, *19*=95-77, *20*=150, *21*=134, *22*=458/6, *23*=458/8, *24*=98-71/1; Karıncalı: *25*=247; Çine: *26*=221/D)

assic to Early Tertiary metabauxite-bearing platform-type marbles, and a metaolistostrome.

The tectono-metamorphic evolution of the Pan-African basement has been mainly attributed to the Alpine (Eocene-Oligocene) metamorphism, termed the "Main Menderes Metamorphism" (Şengör et al. 1984; Dora et al. 1995). Recent studies, as summarized herein, have shown that widespread metagabbroic stocks and veins (Fig. 1) that originally intruded the basement units are important in understanding the tectono-metamorphic evolution of the Menderes Massif (Candan 1994, 1996; Candan et al. 1994; Çetinkaplan 1995; Oberhänsli et al. 1997). These rocks were formerly assigned a Miocene age by Dora et al. (1987). Recent investigations on the metagabbros have revealed that: *(a) the protoliths of the gabbros were Precambrian in age and belong to the Pan-African basement (Candan* 1996*); (b) the gabbros as well as enclosing rocks (i.e., paragneisses and micaschists) experienced multistage metamorphism at granulite-, eclogite-, and amphibolite-facies conditions (Candan et al.* 1994, 1998*; Oberhänsli et al.* 1995, 1997*; Warkus et al.* 1998*); (c) these events were related to the Pan-African orogeny; (d) the effects of Alpine metamorphism on the Pan-African basement should be reevaluated.*

Detailed studies of the metagabbros, which occur throughout the Menderes Massif, are important for the understanding of the high-pressure metamorphism of the Pan-African units (Candan et al. 1994; Çetinkaplan 1995; Oberhänsli et al. 1997). Poorly preserved high-pressure relics in these mafic rocks were first reported in the Birgi and Tire areas (Candan et al. 1994; Çetinkaplan 1995; Oberhänsli et al. 1997). Our studies have revealed the common occurrence of eclogitic metagabbros and relatively fresh eclogites (more than 50 newly discovered outcrops) in the central and northern parts of the Menderes Massif (Fig. 1). Furthermore, the amphibolites in the core series of the Menderes Massif display textural evidence of decompression from high-pressure. This paper reviews the eclogite-facies assemblage in the mafic igneous rocks and subsequent amphibolite-facies conditions during decompression. These high-pressure relics provide important constraints for interpreting tectonic processes that were active during the Pan-African orogeny in western Turkey.

Geological setting of the metagabbros and high-pressure rocks

The widespread occurrence of basic igneous rocks in the Pan-African basement of the Menderes Massif has been known since Önay (1949). Typical lithologies are olivine gabbros, leucogabbros, noritic gabbros, and norites. These rocks are medium- to coarse grained, with subophitic to holocrystalline texture, and locally grade into pegmatitic gabbros. Metagabbros are present in all units of the Pan-African basement, i.e., orthogneisses (augen gneisses, granitic gneisses, and metagranites), charnockitic gneisses, mica schists, and paragneisses. Gabbros generally occur as boudinaged sill-like bodies of several meters in thickness and stocks reaching up to 1500 by 400 m in maximum dimension. They display massive cores and foliated margins that consist mainly of garnet amphibolites. These rocks were extensively deformed and intrusive contact relations have been obliterated.

The first evidence for high-pressure metamorphism in the metagabbros was found in the Tire and Birgi areas (Candan et al. 1994). Coronas and pseudomorphic textures have formed due to the incomplete reactions during the eclogitization. These rocks, referred to as eclogitic metagabbros, were described in detail by Oberhänsli et al. (1997). Field studies and petrographic observations reveal that the transformation from gabbro to eclogitic metagabbro occurred syntectonically and preferentially along distinct shear zones both within the gabbroic bodies and, more typically, along their margins. However, metamorphic reactions during the high-pressure event occurred both within the high-strain zones (eclogitic metagabbros) and in more static low-strain domains (coronitic metagabbros and transient stage rocks). The eclogites were recently discovered for the first time at two localities in the Ödemis-Kiraz Submassif, south of Alasehir and in the Kiraz areas.

In the Kiraz area, the Pan-African basement units are dominated by the partially migmatized paragneisses, and conformably overlying metapelites that comprise of garnet micaschists and biotite–muscovite schist. This Late Proterozoic metapsammitic to metapelitic sequence was intruded by orthogneisses and metagranites following the Pan-African metamorphism (Fig. 2). Mafic rocks occur in the metapelites as sill-like bodies. Around Gökburun, metabasic rocks are almost all garnet amphibolites with the exception of some poorly preserved high-pressure relics. In the northern part of the region, the best-preserved eclogites of the Menderes Massif occur in garnet micaschists as pods and boudinaged layers ranging from 5 to 400 m in long dimension (Fig. 2). Fresh eclogites are massive, medium- to fine-grained rocks. They are characterized by idioblastic garnet crystals embedded in a pale-green groundmass which consists mainly of omphacite. Within micro-shear zones, the eclogites are

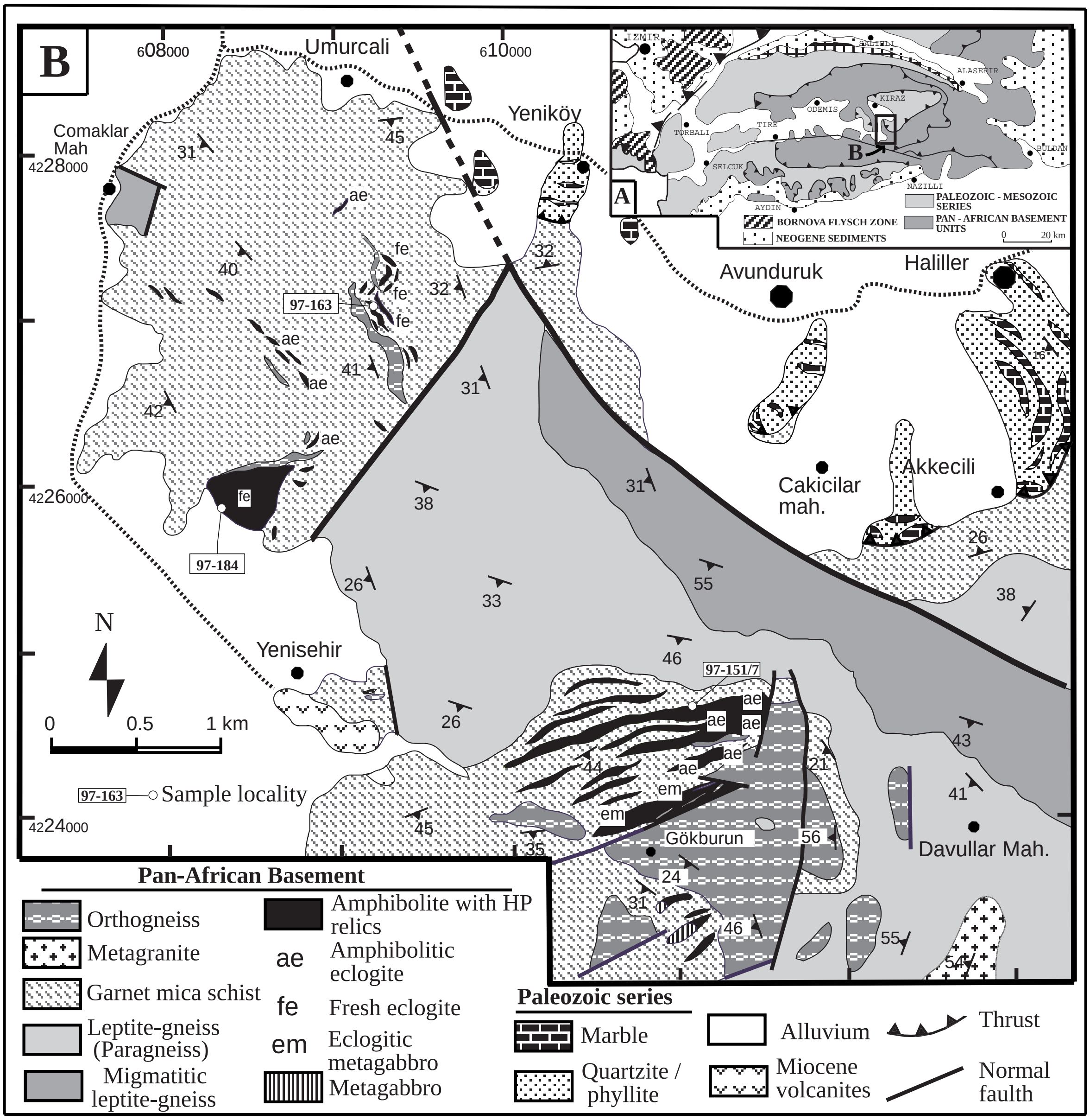

Fig. 2 Geological map of Kiraz region showing the well-preserved eclogites in the Pan-African schists

converted to garnet amphibolites. The foliations of the amphibolite layering in the eclogites and those of the enclosing schist are subparallel. These conditions suggest that the foliation of the country rock developed under amphibolite-facies conditions, and late-stage deformation led to the complete disappearance of high-pressure minerals in the schists.

Another locality for Pan-African high-pressure relics, both eclogites and eclogitic metagabbros, is 8 km southwest of Alasehir (Fig. 3). There, Pan-African basement has been thrusted by the Paleozoic–Mesozoic cover units during the last stage of Late Alpine metamorphism (Partzsch et al. 1998). Furthermore, the Pan-African series also display internal imbrication and can be divided into two tectonic units: (a) a lower tectonic unit which consists mainly of garnet micaschists; and (b) an upper tectonic unit which is dominated by paragneisses intruded by orthogneisses, metagranites, and metabasites. Late Proterozoic garnet micaschists of the lower unit contain numerous garnet-amphibolite lenses reaching up to 10 m in length, but these lack high-pressure relics.

The eclogites, which are restricted to the upper tectonic unit (Fig. 3B), were variably retrograded to garnet amphibolites and occur as dismembered lenses and pods measuring up to 150×30 m. Fresh eclogite has been recognized at only one locality, as a lens measuring 30×5 m. It is a massive, medium-grained rock with typical idioblastic garnet crystals. The eclogite is enclosed by garnet amphibolite. This late-stage alteration has obscured all of the original contact relations of the metabasic rocks. Additionally, the eclo-

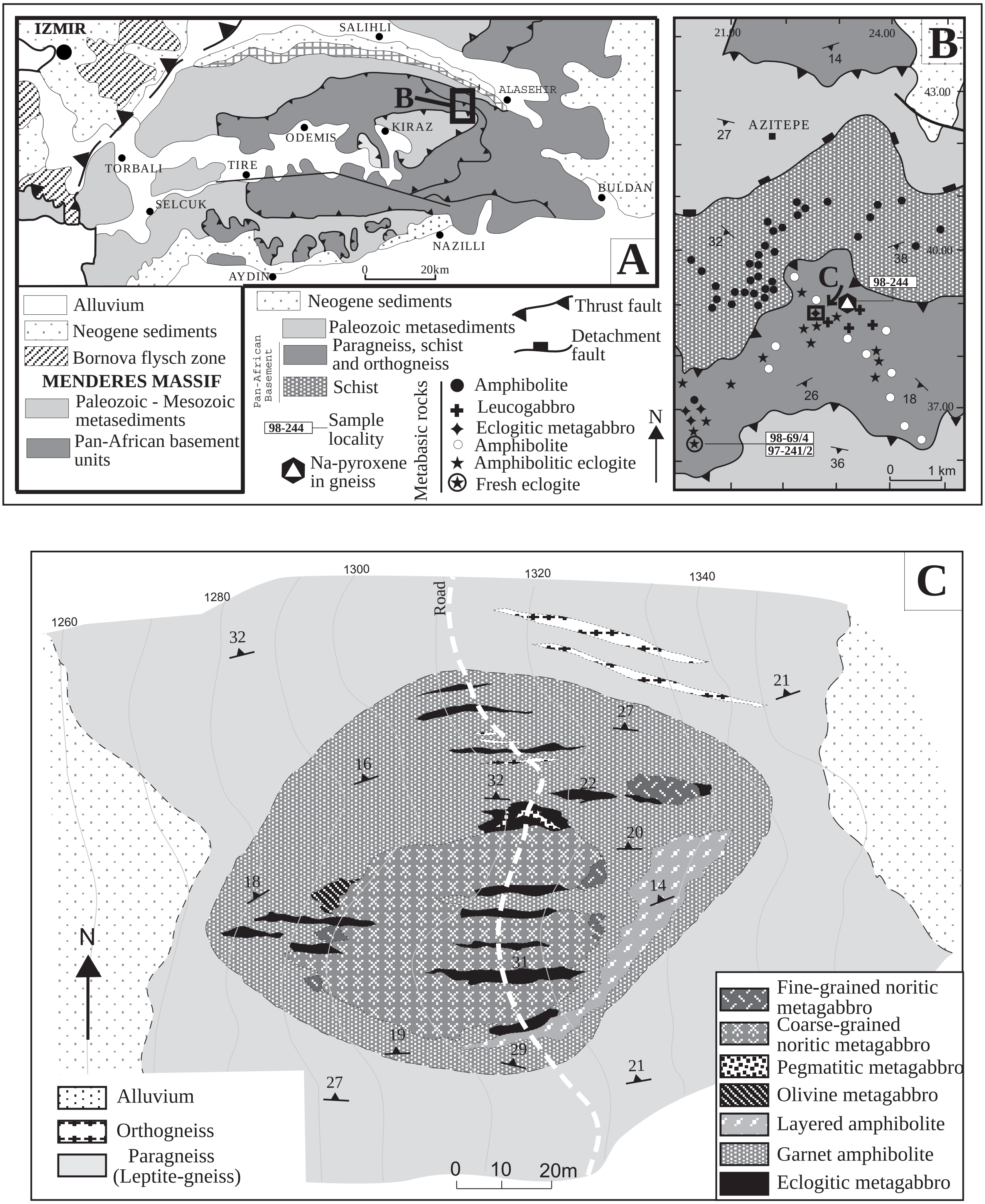

Fig. 3A,B Simplified geological map of Alaşehir region. The high-pressure relics, eclogites and eclogitic metagabbros, are restricted to the upper tectonic unit of the Pan-African basement. **C** Detailed map of an eclogitized noritic metagabbro body in the paragneisses

gitic metagabbros and metanorites were recognized in several localities as stocks and boudinaged layers (Fig. 3C).

In the Menderes Massif, the acidic basement units lack evidence of high-pressure metamorphism but show widespread relics of granulite- and upper-amphibolite-facies conditions. The first direct evidence from the country rocks for in-situ high-pressure metamorphism was discovered in Alasehir (Fig. 3B). At this locality, augen gneisses, which comprise orthoclase porphyroblasts in a strongly deformed groundmass which consists mainly of biotite, garnet, clinopyroxene, and amphibole, enclose eclogites as layers up to 20 cm in thickness. Na-rich clinopyroxenes (max. 12 mol.% Jd) in a biotite-rich groundmass occur as symplectitic intergrowths of clinopyroxene and plagioclase that replace the original omphacitic clinopyroxene.

Petrography

Eclogitic metagabbros

In the massive cores of the gabbroic bodies, the original igneous fabrics characterized by cumulus olivine and plagioclase and intercumulus clino/orthopyroxenes with subophitic to holocrystalline texture are completely preserved. The metamorphic overprint is restricted to minor zoisite occurrences in plagioclase. Based on their mineralogical compositions, these rocks can be subdivided into five groups: olivine gabbro; leuco-gabbro; gabbro; two-pyroxene gabbro (noritic gabbro); and norite. The dominant lithology is gabbro that contains over 65% plagioclase (An 56–72), up to 30% clinopyroxene (augite), but only traces of ilmenite and biotite (Table 1).

The transition from gabbro to eclogitic metagabbro, with a transitional coronite stage, involved a gradual stepwise increase of garnet and omphacite at the expense of igneous plagioclase, ortho/clinopyroxene, and olivine. This occurs variably, ranging from corona development to complete pseudomorphism. The metamorphic reactions during the early stages of the high-pressure overprinting in the basic magmatic rocks are represented essentially by the development of garnet coronas between ferromagnesian phases (ortho/clinopyroxene, ilmenite, and biotite) and plagioclase (Fig. 4a). Garnet crystals extend toward the interiors of the plagioclase domain, and consist of an inner cloudy zone with quartz inclusions and an outer clear zone with idiomorphic terminations. Plagioclase laths are clouded by tiny inclusions of clinozoisite. Kyanite is, in some cases, associated with epidote-group minerals.

Olivine gabbros are characterized by common corona development between olivine and plagioclase. The coronas are made up of successive concentric shells consisting of one or more minerals. An inner shell of orthopyroxene replacing olivine, and an outer zone of Ca–amphibole–spinel symplectitic intergrowth developing inward from the plagioclase, are most common. Occasionally, there is a discontinuous garnet zone embedded in amphibole–spinel zone. Plagioclase is clouded by spinel inclusions which are, in places, sufficiently dense to render the plagioclase opaque. The corona structures between olivine and plagioclase are generally attributed to isobaric cooling after emplacement at depth (Griffen and Heier 1973; Rivers and Mengel 1988). An alternative interpretation, related to the initial stage of eclogitization, which has been suggested to explain the gabbro-eclogite transformation in Norway (Mork 1985) and Canada (Indares 1993), cannot be ruled out for the Menderes coronites. The transition from coronite to eclogitic metagabbro is reflected in the gradual increase of metamorphic minerals, i.e., omphacite and garnet, at the expense of the igneous phases. However, even in the most advanced stage of transformation, relic igneous minerals may persist as metastable phases.

Formation of omphacite

In the transitional samples the Na-clinopyroxenes can be subdivided into two groups: (a) relic intercumulus clinopyroxene; and (b) recrystallized clinopyroxene grains formed by pseudomorphic replacement or as

Table 1 Modal mineralogy (%) and textures of typical samples

		Cpx			Grt		Amp			Pl			Czo	Ky	Bt	Ilm	Rt	Ttn	Qtz	
Texture	Sample	(I)	(R1)	(S)	(C)	(In)	(P)	(R1)	(R2)	(Cu)	(R2)	(lnc)							(lnc)	(R2)
Eclogite																				
Dc	97-184	-	52	9	-	18	-	6	4	-	4	tr	5	-	-	-	2	-	tr	-
Dc	97-163	-	43	15	-	14	-	4	9	-	6	tr	7	-	-	-	2	-	tr	-
Dc	98-694	-	46	16	-	11	-	2	13	-	8	tr	3	-	-	-	1	-	tr	-
Eclogitic metagabbro																				
Dc, Hc, P	97-270/13	22	8	6	8	4	4	-	18	12	4	-	5	2	2	1	2	2	tr	-
Dc, Hc, P	97-120/9	11	16	4	5	9	6	-	22	14	6	-	4	-	-	tr	1	2	tr	-
De, He, P	458/6	28	4	2	9	14	2	-	16	21	2	-	-	-	tr	tr	1	-	tr	-
Garnet amphibolite																				
Dc	97-151/7	-	-	4	-	27	-	-	35	-	22	-	4	-	3	tr	tr	1	tr	4
Dc	98-73/8	-	-	-	-	9	-	-	47	-	23	-	13	-	4	-	-	3	tr	1

Mineral textures are given in parentheses. *R1* recrystallized during high-pressure; *R2* recrystallized during decompression; *I* relic intercumulus phase; *S* symplectite, *C* corona; *In* individual crystal; *P* pseudomorphic replacement; *Cu* relic cumulus phase; *Inc* inclusion in garnet; *Hc* high-pressure corona; *Dc* decompression corona

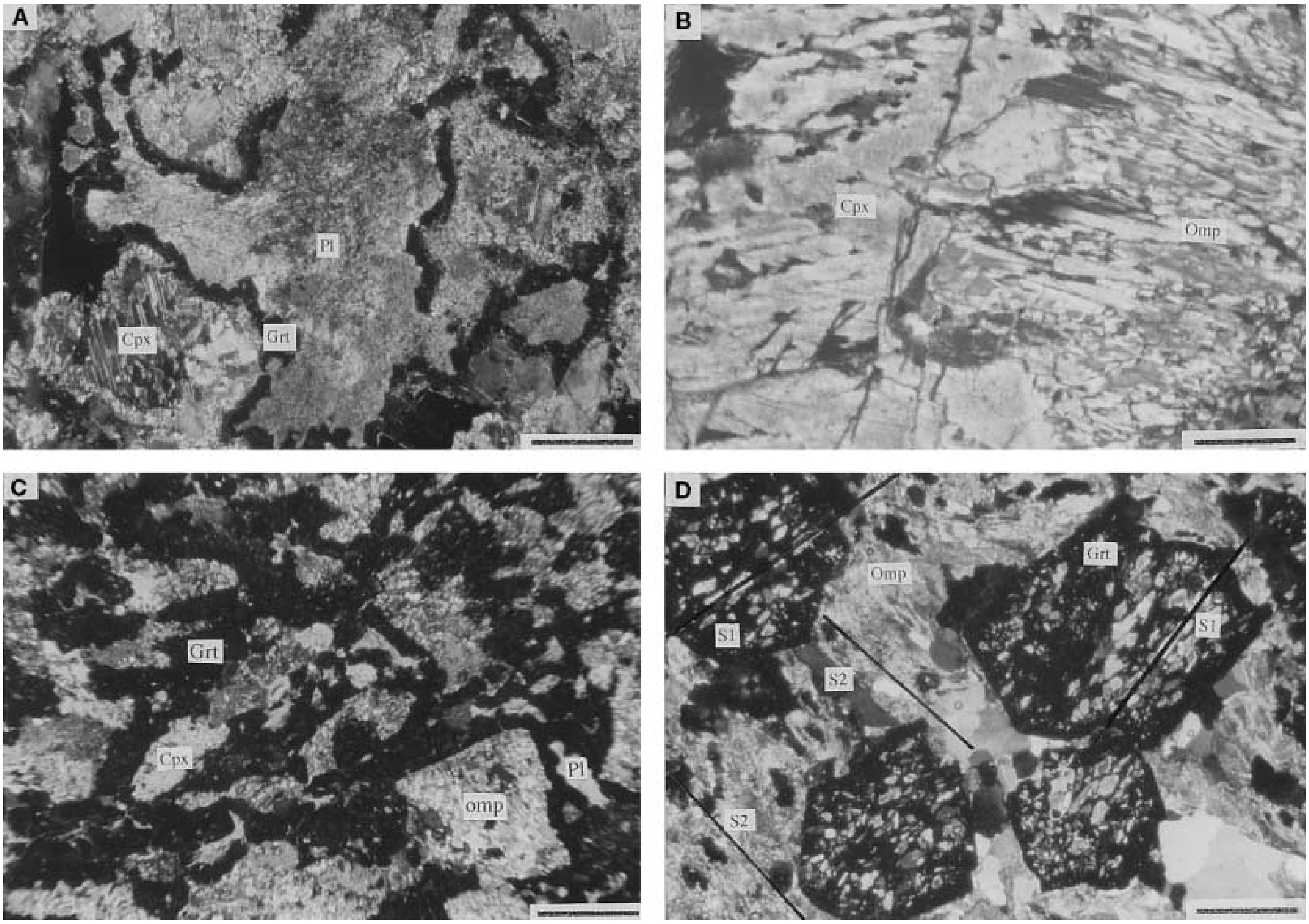

Fig. 4 **A** Garnet coronas developed between igneous clinopyroxene and plagioclase in coronites. **B** Replacement of igneous clinopyroxene by prismatic omphacite crystals. **C** Relic igneous texture in the eclogitic metagabbros. Cumulus plagioclase and intercumulus clinopyroxene are pseudomorphosed by garnet and ompacite, respectively. **D** Inclusion patterns in the garnet porphyroblasts which represent a pre-eclogitic amphibolite facies metamorphism in eclogites. *Cpx* intercumulus clinopyroxene; *Grt* garnet; *Pl* plagioclase; *omp* omphacite. Bars are 200 μm for **A,C,D** and 50 μm for **B**. Sample numbers: **A**=97-120/9; **B**=97-270/13; **C**=95-77, **D**=97-163

corona structures after igneous clinopyroxene (Table 1). Comparison of samples with varying degrees of eclogitization reveals a steady increase in the Jd content of the igneous clinopyroxene with increasing volume of reacted minerals.

Igneous clinopyroxene defines a broad compositional range from sodic augite to omphacite in the transitional rocks, whereas the recrystallized clinopyroxene has a more restricted composition with higher Jd contents. Two groups are recognized: (a) prismatic crystal clusters that pseudomorphically replace the igneous clinopyroxene (Fig. 4b); and (b) granular to polygonal aggregrates surrounding the clinopyroxene as coronas. The same corona structures are also developed around the igneous orthopyroxene in the noritic gabbros and norites.

Pseudomorphism of plagioclase

In the coronites, plagioclase laths contain numerous inclusions of clinozoisite and are isolated from ferromagnesian phases by garnet coronas. During the transitional stage, garnet coronas extend towards the core and some individual idioblastic garnet crystals begin to nucleate within the plagioclase. In the eclogitic metagabbros, the great majority of the plagioclase laths are pseudomorphically replaced by garnet aggregates which preserve the original cumulus texture (Fig. 4c); however, plagioclase is usually not consumed completely and may be present as a relic phase in the central parts of the original plagioclase laths, even in the most advanced stage.

Eclogites

The eclogites generally are more retrograded than the eclogitic metagabbros; however, in some samples, the high-pressure mineralogy is preserved in the domains between microshear zones. The paragenesis in these domains is omphacite–garnet–rutile±clinozoisite±amphibole±quartz (Table 1). The schistosity of the eclogites is defined by the alignment of the prismatic omphacite and clinozoisite crystals. Amphibole generally occurs in coronas around omphacite and symplectites and, therefore, it is often secondary to the eclogite parageneses. However, some individual amphibole crystals are in apparent textural equilibrium with omphacite and garnet with no replacement textures. The inclusions in the core of the garnets are mainly amphibole, titanite, albite, and quartz suggesting that the eclogites were derived by high-pressure prograde metamorphism of medium-pressure protoliths. These inclusions are oriented and reflect an old foliation (S1) which is trapped within the garnet porphyroblasts. This internal fabric transects the main schistosity (S2) of the later high-pressure event (Fig. 4d). The poikiloblastic garnet cores are rimmed by euhedral borders with only a few randomly oriented inclusions of omphacite, quartz, and rutile. This stage represents a period of static growth of garnet under high-pressure conditions.

Fig. 5 **A** Pseudomorphic replacement of omphacite by the symplectitic intergrowth of diopsitic clinopyroxene and plagioclase during the decompression stage. **B** Partial or complete resorption of garnets by plagioclase coronas during the retrograde overprint of eclogites. **C, D** Plagioclase collars which represent de-jateitization of the omphacitic clinopyroxene during decompression in eclogitic metagabbros. *Cpx* intercumulus clinopyroxene; *Grt* Garnet; *Pl (ign.)* igneous plagioclase; *omp* omphacite; *Hb* Hornblende. *Bars* are 200 μm for **B** and **D**, and 50 and 20 μm for **A** and **C**, respectively. Sample numbers: **A**=97-184; **B**=98-71/1; **C**=96-127/3; **D**=96-127/3

Decompression textures

Both the eclogite and eclogitic metagabbro are strongly retrograded. Omphacite is commonly replaced by a fine-grained vermicular intergrowth of clinopyroxene (Jd 14) and plagioclase (An 8–11), similar to that observed in other eclogites (Fig. 5a; e.g., De Wit and Strong 1975; Okay et al. 1985; Baker 1986). In the advanced stages, hornblende crystals have replaced the clinopyroxene in the symplectite. Garnet in the retrograded eclogites is typically resorbed by plagioclase coronas (Fig. 5b). Minor hornblende also occurs as vermicular intergrowths oriented radially to the garnet boundary. The resorption of garnet is interpreted to reflect a decrease in pressure during the retrogression of the eclogites (Baker 1986; Wilkerson et al. 1988). Plagioclase collars between relic igneous and high-pressure phases, which are

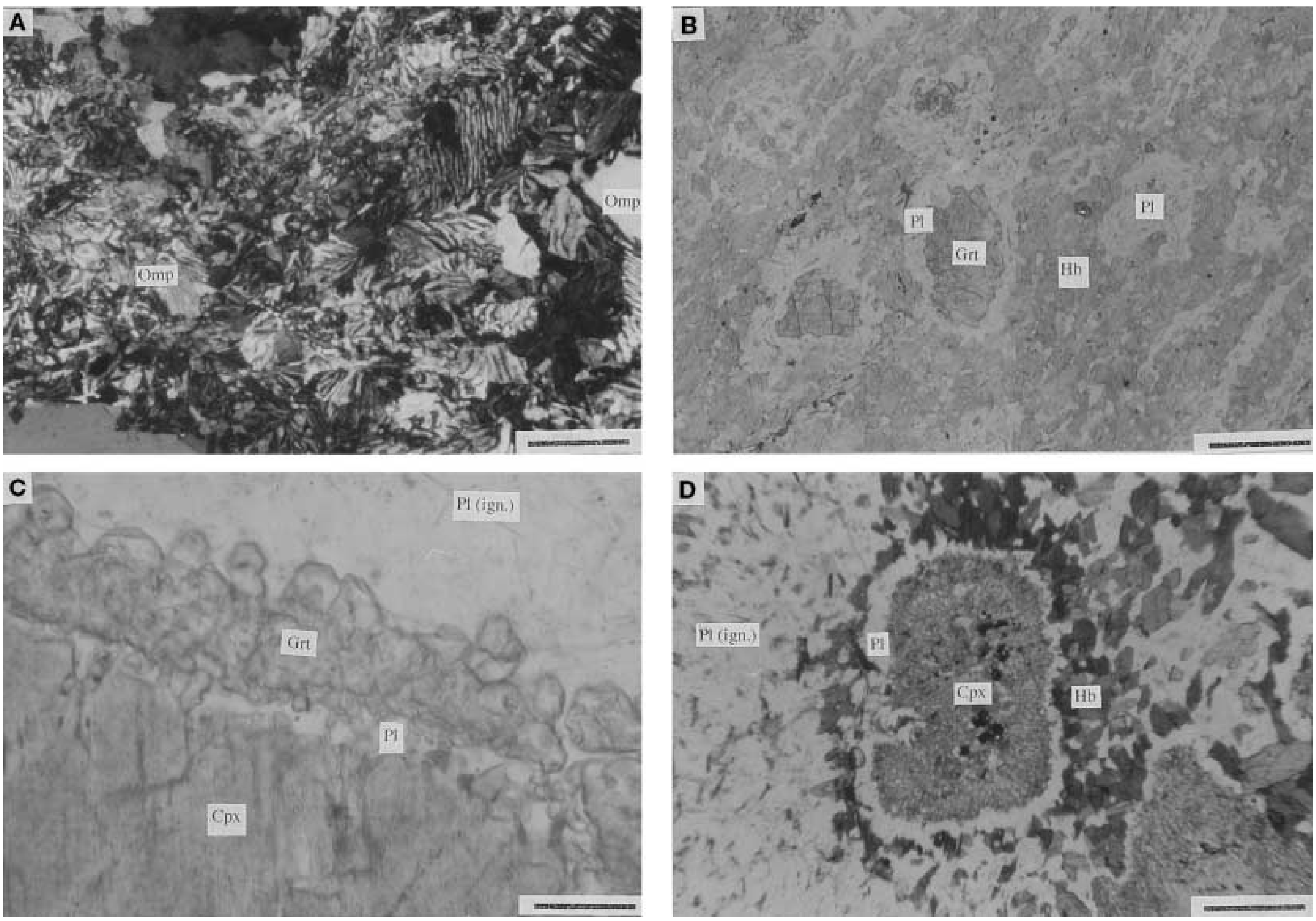

regarded to be related to de-jadeitization of adjacent clinopyroxene during decompression of high-pressure rocks (Indares 1993), are extensively developed in the coronites and eclogitic metagabbros. This corona texture can be divided into two groups: (a) plagioclase collars separating garnet coronas developed during the progressive eclogitization from sodic clinopyroxene (Fig. 5c); and (b) plagioclase collars between sodic clinopyroxene and relic igneous plagioclase (Fig. 5d). In the second type, plagioclase collars are enclosed by bluish-green amphibole outer shells, extending radially into plagioclase.

Mineral chemistry

Four samples typical of the eclogites, ten samples of coronites and eclogitic metagabbros, four samples of metagabbro, eleven samples of garnet amphibolites and one sample of clinopyroxene-bearing gneiss, were chosen for microprobe analysis (Fig. 1). Analyses were performed on three different electron microprobes, Camebax and Jeol 8900 units in Mainz, and a Jeol 8800 unit in the Humboldt Museum (Berlin, Germany) using natural and synthetic standards.

Clinopyroxene

The intercumulus clinopyroxene in the well-preserved gabbroic rocks is augitic in composition. The Na contents of the clinopyroxene in these rocks, which are not affected by the corona-forming reactions, range from 0.27 to 0.81 wt.% Na_2O (1–3 mol.% Jd) with an average value of approximately 0.48 wt.% Na_2O. The intergrain chemical variation of the intercumulus clinopyroxene is related to the degree of consumption of plagioclase and shows a regular rimward increase in Jd content. The average Jd contents of the clinopyroxene, which preserves its original igneous forms in the coronites, range from 7.3 to 9.7 mol.% and concentrate in the Na–augite field (Fig. 6). However, in the same rocks, the recrystallized clinopyroxene has higher Jd contents, ranging from 12.0 to 22.7 mol.% Jd (Tables 2 and 3) and plots in the Na–augite and omphacite fields (Fig. 6). In the advanced stages of transformation, the Jd contents of the intercumulus clinopyroxene increase steadily and reach up to 36.4 mol.% in the eclogitic metagabbros.

Clinopyroxene in the fresh eclogites has homogeneous composition. The Jd contents range from 42.05 to 50.4 mol.% and concentrate in the omphacite field;

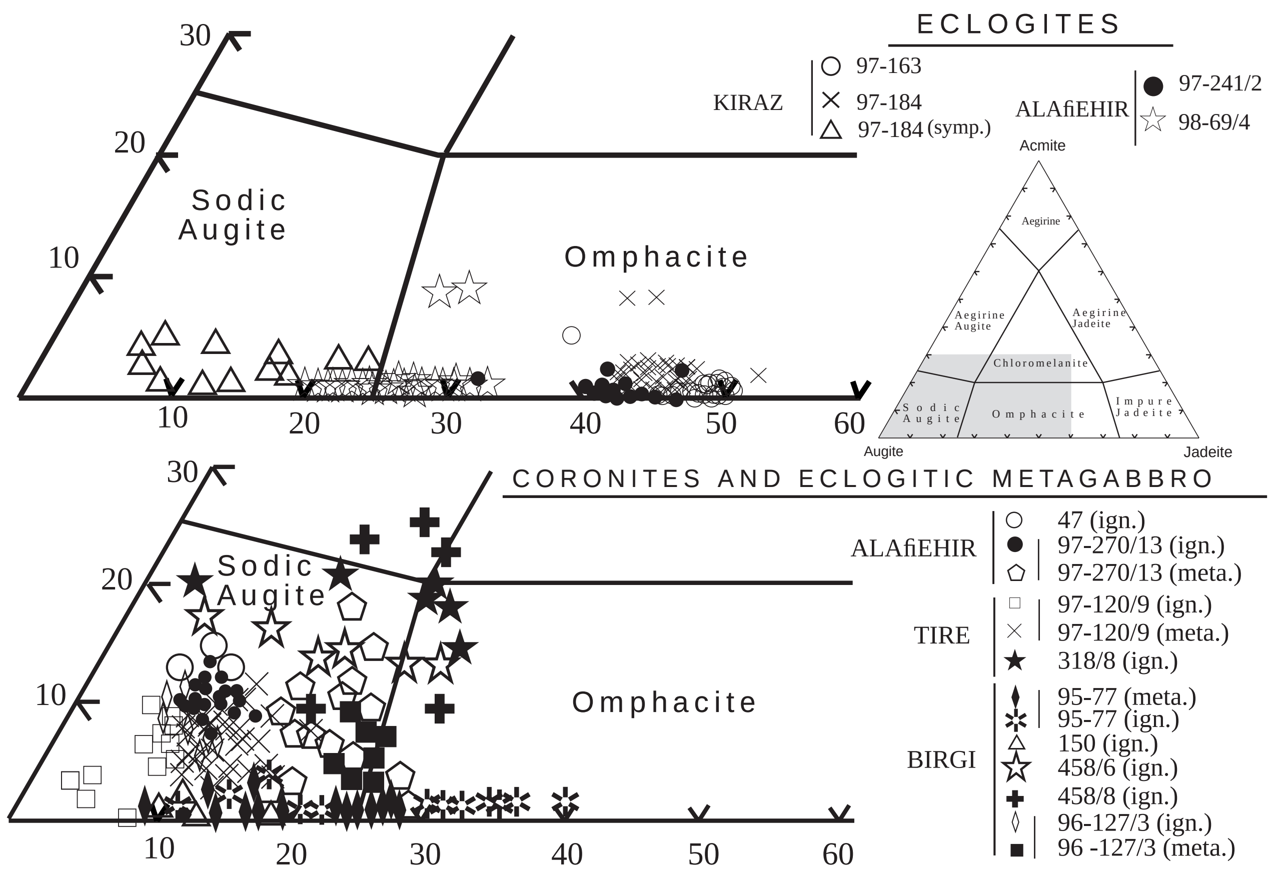

Fig. 6 Clinopyroxene composition from the Menderes eclogites and eclogitic metagabbros plotted on jadeite–acmite–Na–augite diagram. (After Essene and Fyfe 1967)

Table 2 Representative clinopyroxene analyses from eclogites, eclogitic metagabbros, and gneisses

	Eclogite				Eclogite metagabbro			Gneis
					recrystalized	intercumulus		
	Symplectite	omp	omp	omp		Core	Rim	
	80	76	185	31	101	146	108	163
Sample	97-184	97-184	97-163	97-241	96-77	96-77	96-77	97-224
SiO_2	54.02	55.86	56.48	57.03	54.53	54.34	54.78	52.78
TiO_2	0.00	0.02	0.13	0.05	0.12	0.10	0.08	0.00
Al_2O_3	1.97	10.88	11.88	11.61	5.30	2.58	6.89	2.27
FeO	8.30	4.82	3.94	3.16	5.28	5.30	4.61	13.90
MnO	0.05	0.12	0.11	0.00	0.06	0.03	0.01	0.08
MgO	12.52	8.23	7.74	8.25	12.10	13.61	11.05	9.07
CaO	21.59	13.65	12.86	14.05	19.63	21.62	17.91	17.73
Na_2O	1.65	6.49	6.69	6.49	2.69	1.49	3.96	2.79
K_2O	0.01	0.01	0.00	0.02	0.00	0.00	0.00	0.01
Cr_2O3	0.02	0.01	0.04	0.16	0.12	0.22	0.12	0.01
Total	100.15	100.14	99.91	100.85	99.84	99.30	99.43	98.72
Si	1.994	1.989	2.011	2.010	1.988	2.005	1.987	2.007
Al (IV)	0.006	0.011	0.000	0.000	0.012	0.000	0.013	0.000
Total	2.000	2.000	2.011	2.010	2.000	2.005	2.000	2.007
Al (VI)	0.080	0.446	0.499	0.482	0.216	0.112	0.282	0.102
Fe^{2+}	0.212	0.131	0.117	0.093	0.161	0.163	0.133	0.340
Fe^{3+}	0.045	0.013	0.000	0.000	0.000	0.000	0.007	0.104
Mg	0.663	0.410	0.379	0.418	0.616	0.715	0.572	0.454
Ti	0.000	0.001	0.004	0.001	0.003	0.003	0.002	0.000
Cr	0.001	0.000	0.001	0.005	0.004	0.007	0.004	0.000
Total	1.000	1.000	1.000	1.000	1.000	1.000	1.000	1.000
Na	0.118	0.448	0.462	0.443	0.190	0.107	0.696	0.723
Mg	0.026	0.027	0.032	0.015	0.041	0.034	0.025	0.061
Total	0.998	0.996	0.985	0.989	0.998	0.995	1.000	0.989
Jd	8.1	45.5	50.4	47.6	21.9	11.6	28.6	10.9
Ac	4.5	1.3	0.0	0.0	0.0	0.0	0.7	11.1
Au	87.3	53.1	49.5	52.3	78.0	88.3	70.6	77.8

however, in altered samples, the Jd contents decrease to approximately 29.5 mol.%. Secondary clinopyroxene replaces the omphacite during decompression and has distinctly low Jd contents ranging from 8.1 to 19.2 mol.%, and plots in the Na–augite field (Fig. 6). Clinopyroxene in gneisses is mostly retrograded to symplectitic intergrowths. In less altered grains, the Jd content ranges from 9.5 to 11.8 mol.%.

Garnet

The compositional ranges of garnet from the eclogites, eclogitic metagabbros, and garnet amphibolites are illustrated on the alm+sps–pyp–grs+and ternary diagram (Fig. 7). In the eclogites, idioblastic garnet crystals show distinct chemical zoning (Table 4). Grossular content decreases regularly toward the rim from 25.0 to 21.7 mol.%, and pyrope content increases from 15.9 to 21.2 mol.% (Fig. 8A). When combined with the amphibolite-facies inclusions in their cores, the growth-zoning profiles in garnet could be interpreted as a result of prograde crystallization from amphibolite- to eclogite-facies conditions at a slow rate of volume diffusion (Krogh 1982).

Garnet crystals in the eclogitic metagabbros can be divided texturally into two groups: (a) corona garnet; and (b) idioblastic individual garnet. The garnet coronas show distinct zoning, always with the highest Ca contents close to adjacent relic igneous plagioclase. Grossular contents increase from 20.5 to as much as 22.2 mol.% toward the plagioclase, and pyrope and almandine contents decrease rimward from 28.3 to 24.8 mol.%, and from 50.2 to 49.0 mol.%, respectively (Fig. 8B). Idioblastic garnet crystals in plagioclase have chemically homogeneous compositions with almost flat profiles (Fig. 8C). The average composition of this pyrope-poor garnet is Alm 59.9–Prp 13.9–Sps 1.5–Grs 23.9–And 0.8 (Fig. 7). The chemical compositions of this garnets are similar to those garnets in the amphibolites (average composition: Alm 57.7–Prp 14.3–Sps 1.6–Grs 26.1–And 0.4). This similarity suggests that some of the garnets in the retrograded eclogitic metagabbros could have crystallized during the Barrovian-type overprinting metamorphism.

Garnet in the amphibolites can be classified into two groups in terms of their Mg contents: (a) Mg-rich garnet (pyrope contents between 22 and 28 mol.%); and (b) Mg-poor garnets (pyrope contents between 12 and 17 mol.%) with flat zoning profiles. The pyrope-rich garnets are believed to be relic from the high-pressure stage, whereas the pyrope-poor garnet apparently formed during Barrovian overprinting.

Table 3 Representative clinopyroxene and amphibole analyses from eclogites, eclogitic metagabbros, and garnet amphibolite

	Eclogite			Eclogite metagabbro		Garnet amphibolite	
	Na–Ca amp		Ca amp	Ca amp		Ca amp	
Sample	254 97-163	93 97-184	58 97-241/2	18 97-127/3	164 96-77	98 98-71/1	72 98-73/8
SiO_2	49.91	48.13	53.80	41.13	41.02	44.06	42.74
TiO_2	0.42	0.34	0.06	0.92	0.56	0.63	0.76
Al_2O_3	12.93	11.02	1.68	13.24	18.27	15.17	15.09
FeO	13.12	10.64	15.39	20.31	10.97	10.33	16.13
MnO	0.09	0.08	0.54	0.03	0.00	0.12	0.10
MgO	12.09	14.88	13.84	8.09	11.25	13.04	9.36
CaO	7.52	8.07	12.47	10.82	11.76	11.52	11.44
Na_2O	4.64	4.56	0.17	2.24	2.10	1.56	1.47
K_2O	0.31	0.26	0.09	1.44	1.67	0.99	0.63
Cr_2O3	0.01	0.00	0.00	0.00	0.00	0.10	0.03
Total	98.08	98.01	98.05	08.22	97.60	97.13	97.75
T:Si	6.661	6.761	7.789	6.182	5.997	6.137	6.268
Al (IV)	1.339	1.239	0.211	1.818	2.003	1.683	1.732
Fe^{3+}	0.000	0.000	0.000	0.000	0.000	0.000	0.000
Ti	0.000	0.000	0.000	0.000	0.000	0.000	0.000
T-Total	8.000	8.000	8.000	8.000	8.000	8.000	8.000
C:Al (VI)	0.825	0.586	0.077	0.527	1.146	0.880	0.876
Ti	0.045	0.037	0.006	0.104	0.062	0.069	0.084
Fe^{3+}	0.797	0.860	0.188	0.669	0.143	0.574	0.554
Cr	0.000	0.000	0.000	0.000	0.000	0.012	0.003
Mg	2.560	3.117	2.987	1.301	1.350	1.534	1.518
Fe^{2+}	0.761	0.391	1.676	1.812	2.451	2.786	1.046
Mn	0.011	0.010	0.066	1.884	1.198	0.664	1.424
Ca	0.000	0.000	0.000	0.003	0.000	0.015	0.012
C-Total	5.000	5.000	5.000	5.000	5.000	5.000	5.000
B:Ca	1.145	1.215	1.934	1.742	1.842	1.769	1.797
Na	0.855	0.785	0.048	0.258	0.158	0.231	0.203
B-Total	2.000	2.000	1.982	2.000	2.000	2.000	2.000
A:Ca	0.000	0.000	0.000	0.000	0.000	0.000	0.000
Na	0.424	k0.458	0.000	0.395	0.437	0.203	0.215
K	0.057	0.047	0.017	0.276	0.311	0.108	0.118
A-Total	0.481	0.505	0.017	0.671	0.749	0.311	0.333

Amphibole

Based on textural evidence, two groups of amphibole are found in the eclogites. Brownish-green amphibole aligned parallel to the main foliation is texturally in equilibrium with high-pressure phases and display no reaction rims or replacement textures. The Na contents of these minerals range from 4.0 to 4.7 wt.% Na_2O (Table 3). According to Leake et al. (1997), these are sodic–calcic amphiboles with Na_B values varying between 0.68 and 0.78 and plot in the barroisite and magnesio-katophorite fields. In the discrimination diagrams of Laird and Albee (1981), these amphiboles are clearly separated from the post-eclogitic amphiboles and are concentrated in the field of intermediate- to high-pressure facies amphiboles (Fig. 9). In the retrograded eclogites, bluish-green amphiboles around garnet crystals and in the matrix (the second group) are calcic amphiboles and have highly variable compositions between edenite and pargasite (Fig. 10).

The amphiboles in the eclogitic metagabbros are secondary calcic amphiboles replacing sodic-clinopyroxene and relic igneous plagioclase. Although the compositions of these amphiboles are highly variable, they mainly concentrate in the tschermakite and hastingsite fields (Fig. 10). Bluish-green amphibole in the coronas between relic plagioclase and clinopyroxene is hastingsite with Na_2O contents up to 3.9 wt.%. Dark-green amphibole replacing both omphacite and symplectitic clinopyroxene in the altered eclogitic metagabbros is tschermakite (Fig. 10).

Amphiboles are the dominant phase in the garnet amphibolites and occur as prismatic crystals aligned parallel to the main foliation. These amphiboles mainly plot in the magnesio-hornblende to tschermakite and ferroan pargasite fields (Fig. 10). The calcic amphiboles from the eclogites, eclogitic metagabbros, and garnet amphibolites, except for the sodic-calcic amphiboles in the eclogites, plot in the low-pressure part of the diagrams of Laird and Albee (1981; Fig. 9), and are consistent with a post-eclogitic origin for these minerals.

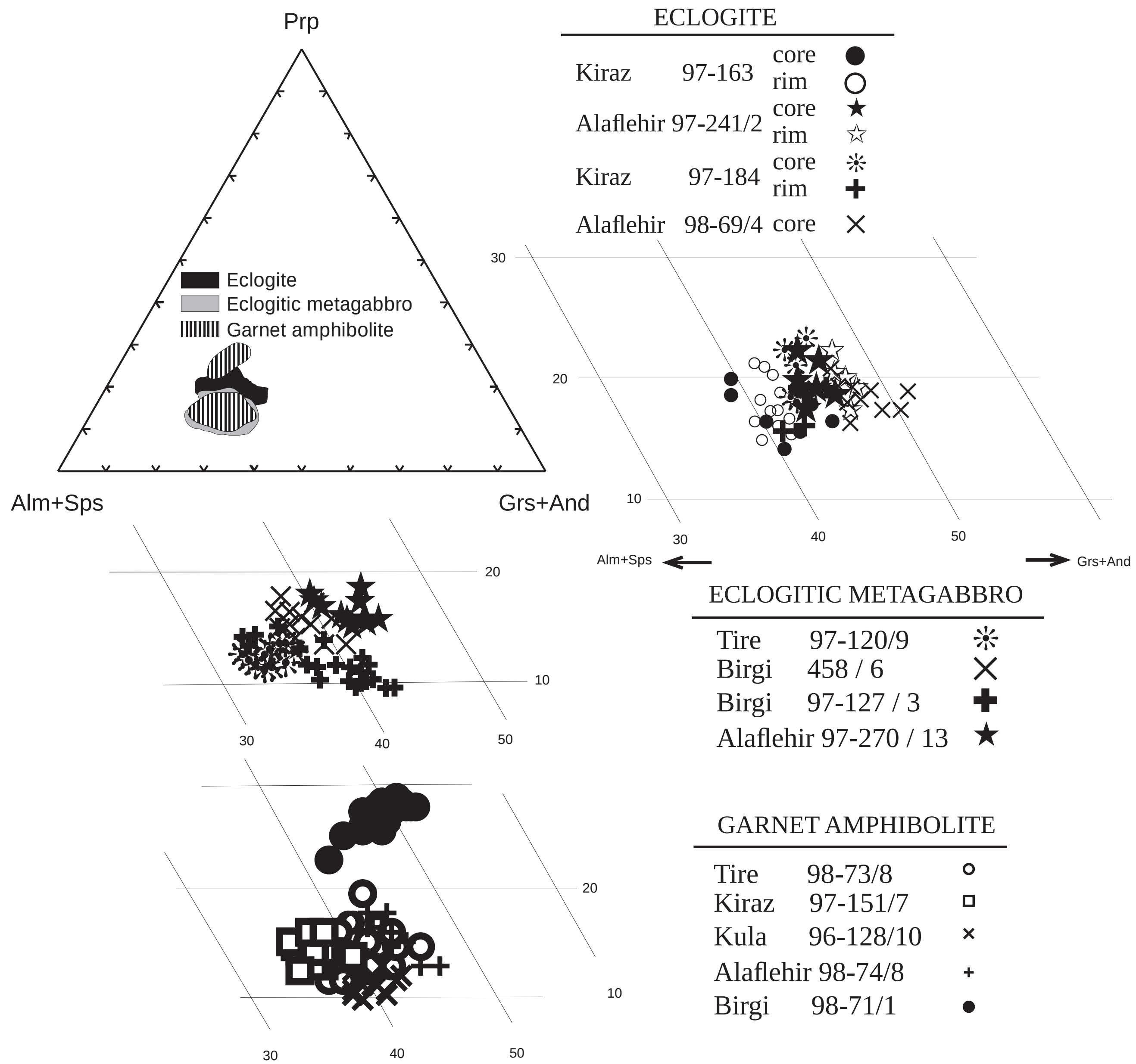

Fig. 7 Triangular diagram pyrope–almandine+spessartine–grossular+andradite for garnets from eclogites, eclogitic metagabbros, and garnet-amphibolites of the Menderes Massif

Pressure–temperature estimations

Temperature estimations

The Fe^{2+}-Mg exchange between garnet and clinopyroxene can be used to estimate the temperature of high-pressure metamorphism for eclogites and eclogitic metagabbros. The temperature values calculated for the eclogites after Krogh (1988) and Ellis and Green (1979) exhibit reasonable results with mean values of approximately 596 and 644 °C, respectively, at 15 kbar (Fig. 11; Table 5). The values confirm the difference of approximately 50 °C between these two calibrations as emphasized by Krogh (1988) and Rahn (1991). One hundred six clinopyroxene–garnet pairs from four samples were plotted into a histogram to compare the spread of temperatures calculated by Ellis and Green (1979) and Krogh (1988). Temperatures calculated by Krogh (1988) exhibit a considerable spread, ranging from 505 to 685 °C, whereas the data sets for the Ellis and Green (1979) calibration are more concentrated, restricted in the range of 565 and 700 °C, yielding a distinct peak temperature between 640 and 665 °C (Fig. 12).

The garnet–clinopyroxene geothermometer in the eclogitic metagabbros exhibits a considerable spread of temperature values due to incomplete reactions, common corona formation, distinct chemical zoning in

Table 4 Representative garnet analyses from eclogites, eclogitic metagabbros and garnet-amphibolites

	Eclogite				Eclogitic metagabbro			Garnet-amphibolite			
Sample	Core 97-163	Rim 97-163	Core 97-184	Rim 97-184	Corona 95-77	Core 95-77	Rim 95-77	Core 98-71/1	Rim 98-71/1	Core 98-73/8	Rim 98-73/8
SiO_2	39.45	39.59	38.38	38.95	38.76	38.92	38.45	39.35	39.16	38.86	38.70
TiO_2	0.14	0.04	0.20	0.04	0.21	0.12	0.08	0.07	0.00	0.17	0.04
Al_2O_3	22.32	22.55	21.51	21.75	21.22	21.34	21.43	22.13	22.11	21.32	21.94
FeO	27.50	27.07	27.22	25.48	29.97	30.45	29.92	24.61	25.36	27.49	26.41
MnO	0.50	0.35	0.66	0.45	0.89	0.85	0.98	0.92	1.136	0.77	0.39
MgO	4.22	5.65	3.84	5.97	3.24	3.39	3.47	6.86	6.67	3.80	3.94
CaO	9.35	8.15	9.29	8.60	8.35	7.61	7.99	7.70	7.23	9.03	10.01
Na_2O	0.06	0.01	0.08	0.00	0.09	0.10	0.05	0.04	0.00	0.02	0.00
K_2O	0.00	0.00	0.00	0.00	0.00	0.00	0.00	0.00	0.00	0.00	0.00
Cr_2O_3	0.01	0.00	0.00	0.00	0.03	0.02	0.00	0.00	0.01	0.01	0.01
Total	103.59	103.45	101.23	101.26	102.77	102.82	102.38	101.69	101.68	101.48	101.45
Mg	0.954	1.270	10891	1.367	0.747	0.781	0.803	1.555	1.517	0.879	0.908
Mn	0.064	0.045	0.088	0.059	0.117	0.112	0.129	0.118	0.147	0.102	0.051
Ca	1.518	1.316	1.550	1.416	1.384	1.260	1.392	1.255	1.182	1.501	1.657
Fe (II)	3.464	3.368	3.471	3.158	3.751	3.847	3.739	3.072	3.154	3.519	3.384
Total X	6.000	6.000	6.000	6.000	6.000	6.000	6.000	6.000	6.000	6.000	6.000
Rest Fe	0.021	0.044	0.071	0.115	0.127	0.088	0.146	0.058	0.082	0.048	0.029
Si	5.977	5.967	5.973	5.983	5.999	6.016	5.971	5.984	5.976	6.029	5.981
Al (IV)	0.023	0.033	0.027	0.017	0.001	0.000	0.029	0.016	0.024	0.000	0.019
Total Z	6.000	6.000	6.000	6.000	6.000	6.016	6.000	6.000	6.000	6.000	6.000
Al (VI)	3.962	3.974	3.920	3.922	3.870	3.888	3.893	3.952	3.953	3.899	3.978
Cr	0.002	0.000	0.000	0.000	0.004	0.002	0.000	0.000	0.001	0.001	0.002
Ti	0.017	0.005	0.024	0.006	0.025	0.015	0.010	0.008	0.000	0.020	0.005
Fe (III)	0.021	0.044	0.071	0.115	0.127	0.088	0.146	0.058	0.082	0.048	0.029
Total Y	4.002	4.022	4.016	4.042	4.025	3.993	4.049	4.017	4.035	3.968	4.014
Alm (%)	57.7	56.1	57.9	52.6	62.5	65.1	62.3	51.2	52.6	58.6	56.4
Prp (%)	15.9	21.2	14.8	22.8	12.5	13.0	13.4	25.9	25.3	14.6	15.1
Sps (%)	1.1	0.7	1.5	1.0	1.9	1.9	2.1	2.0	2.4	1.7	0.9
Grs (%)	25.0	21.7	25.2	22.9	22.2	20.4	21.3	20.6	19.3	24.6	27.4
And (%)	0.2	0.3	0.6	0.7	0.9	0.5	0.9	0.3	0.4	0.4	0.2

Table 5 The *P–T* estimations from eclogites and eclogitic metagabbros

			Grt/Cpx thermometer		Jd–Al–Q barometer
			Krogh (1988)	Ellis and Green (1979)	Holland (1980)
Eclogite					
Kiraz	97-184	Omp	581	629	14.8
		Omp/Grt core	581	630	-
		Omp/Grt rim	586	634	-
		Symp. Cpx	580	629	8.9
	97-163	Omp	611	565	15
Alaşehir	98-69/4	Omp	611	656	14.6
		Symp. Cpx	610	654	-
	96-241/2	Omp	595	643	15.1
		Omp/Grt core	592	642	-
		Omp/Grt rim	598	645	-
Average values (°C, kbar)		omph	596	644	14.9
		symp.	595	642	8.9
Eclogitic metagabbro					
Birgi	458/6		523	579	12.2
	548/8		647	692	12.0
	134		631	672	11.8
	150		521	581	10.4
	96-127/3		626	674	-
	95/77		613	668	11.8
Tire	96-120/9		512	582	-
	318/8		571	616	11.9
Average values (°C, kbar)			581	633	11.7

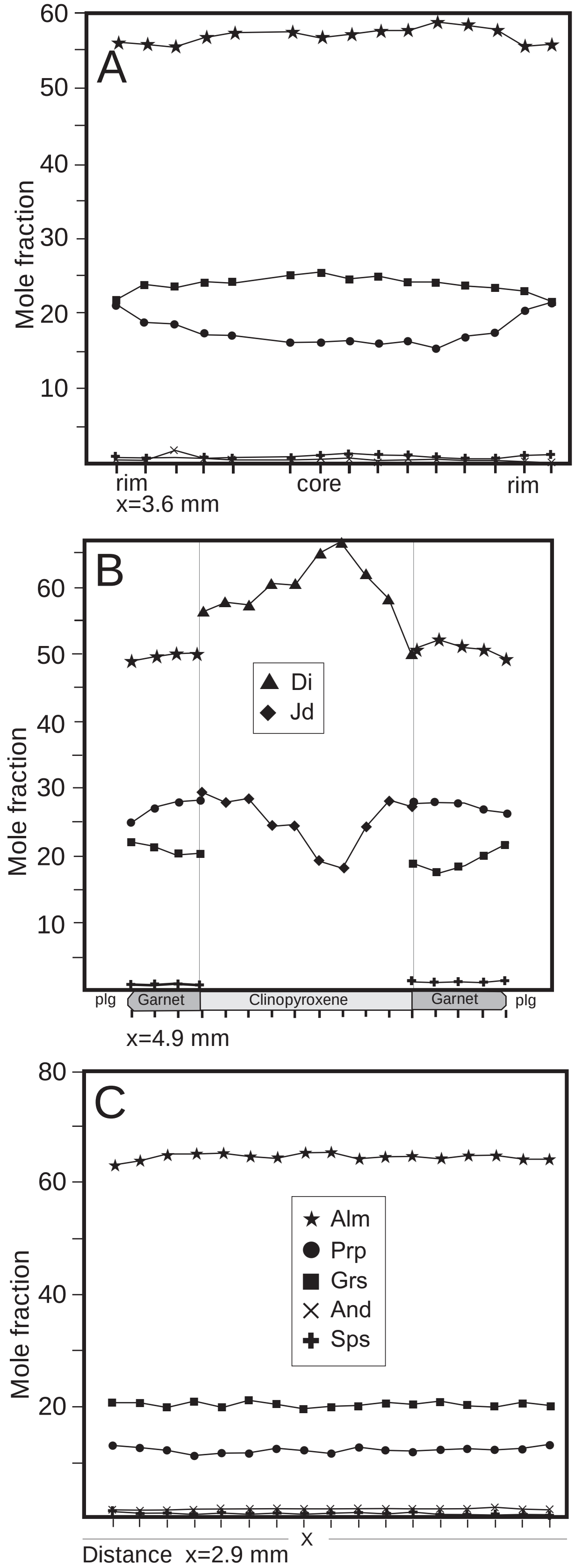

Fig. 8 **A** Typical zoning profile of idioblastic garnet crystal in eclogites. **B** Chemical zoning of corona garnets between intercumulus clinopyroxene and igneous plagioclase. As a result of the replacement of igneous plagioclase by garnet coronas during high-pressure metamorphism, jadeite content increases from the core of the intercumulus clinopyroxene (Jd_{18}) toward the rim (Jd_{30}). **C** Flat chemical profile in the idioblastic garnet crystals in the eclogitic metagabbros. Sample numbers: **A**=97-184; **B**=97-120/9; **C**=97-120/9

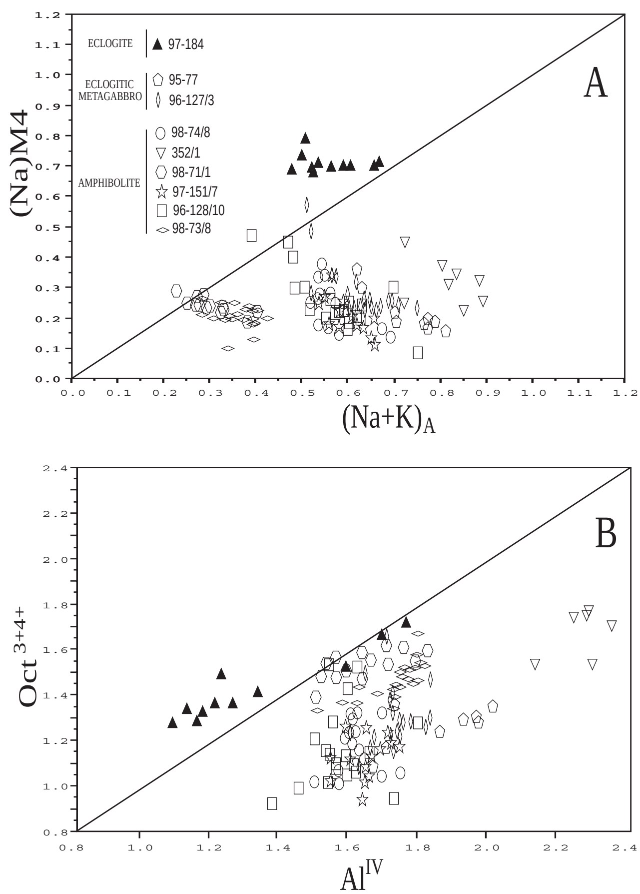

Fig. 9A,B Amphibole composition diagrams from eclogites, eclogitic metagabbros, and garnet amphibolites plotted on the Laird and Albee (1981) diagrams. Note that the amphiboles which are texturally in equilibrium with high-pressure phases (*black triangles*) clearly plot in the intermediate- to high-pressure facies series

minerals, and the persistence of relic igneous phases (Fig. 11; Table 5). The Ellis and Green (1979) calibration yields a mean value of approximately 633 °C at 12 kbar. Although the mean temperature value is very similar to that of the eclogites, the difference between maximum and minimum values is much larger (eclogites: 27 °C; eclogitic metagabbros: 151 °C; Table 5).

Garnet–biotite, garnet–hornblende, and amphibole–plagioclase geothermometers were used to estimate temperature in the amphibolites (Table 6). Eighteen calibrations for biotite–garnet pairs were applied to

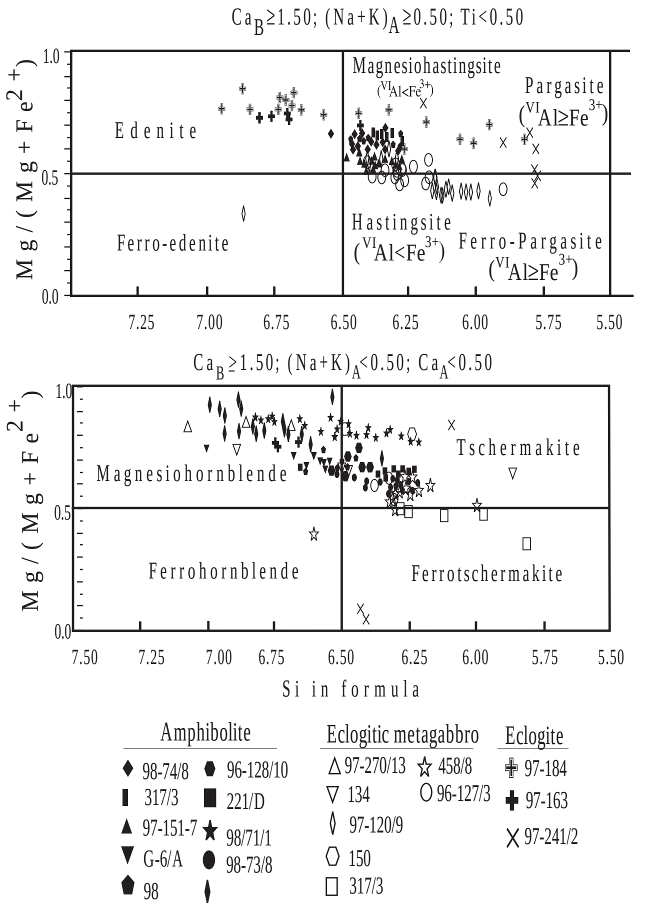

Fig. 10 Composition of Ca-amphiboles from eclogite, eclogitic metagabbros, and garnet amphibolites shown in the Mg/Mg+ Fe^{2+} vs Si diagrams. (After Leake et al. 1997)

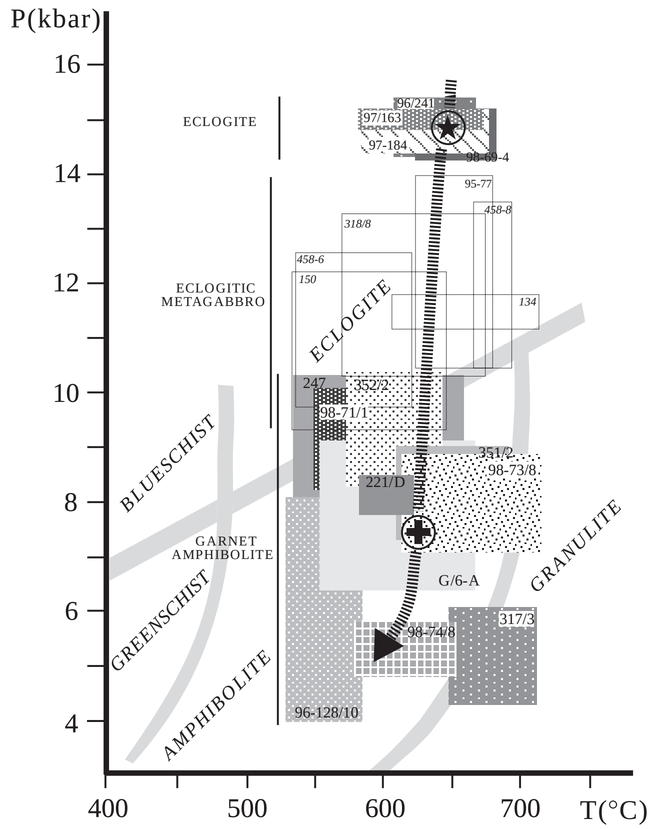

Fig. 11 Pressure–temperature estimations of the eclogites, eclogitic metagabbros, and garnet amphibolites. *Star* and *cross* represent the mean *P–T* values of eclogites and amphibolites, respectively. Petrogenetic grid is after Krogh (1982)

the data sets, and 10 of them yielded reasonable results with a mean value of approximately 622 °C at 7 kbar. The calibrations of Ferry and Spear (1978), Perchuk and Lavrent'eva (1983), and Bhattacharya et al. (1992) especially exhibit similar results with an average value of approximately 623 °C (Table 6). The garnet–hornblende Mg–Fe exchange geothermometer of Graham and Powell (1984) gave temperature estimates of approximately 611 °C at 7 kbar, which agree reasonably well with the results from the garnet–biotite pairs (Table 6).

Pressure estimations

The metamorphic pressures of the eclogites were estimated using the albite=jadeite+quartz barometer (Holland 1980). Since omphacite coexists with quartz

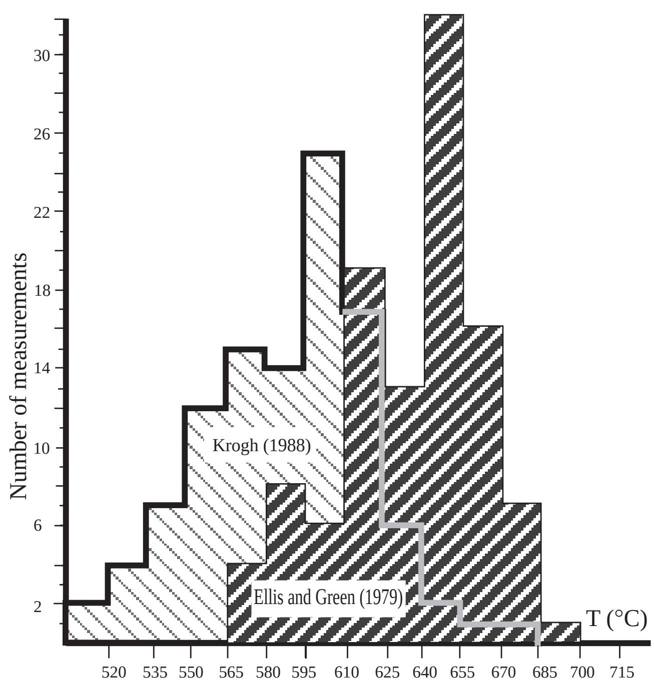

Fig. 12 Histogram of the calculated metamorphic temperatures from the garnet-clinopyroxene Mg-Fe geothermometer at a pressure 15 kbar for two different calibrations

Table 6 The *P-T* estimations from garnet-amphibolites. *c* core; *r* rim; *m* matrix

		Biotite/garnet geothermometer			Hornblende/garnet geothermometer	Hbi–Pt–Grt–Q geobarometer
		Ferry and Spear (1978)	Perchuk and Lavrent'eva (1983)	Bathacharya et al. (1992)	Graham and Powell (1984)	Krohn and Spear (1989)
Birgi	98	-	-	-	611	7.7
	98-71/1					
	Grt (c)–Bt (m)	624	611	625	549	9.5
	Grt (r)–Bt (m)	640	619	636		
Tire	317/3	-	-	-	675	5.1
	98-73/8	-	-	-	632	7.7
Alaşehir	98-74/8	580	586	615	622	4.9
Kiraz	97-151/7	601	598	616	613	5.3
Kula	G-6/A	-	-	-	612	8.3
	96-128/10	-	-	-	572	5.3
Salihli	352/2	625	611	634	588	9.2
	351/2	712	647	662	701	8.0
Karıncalı	247	-	-	-	568	9.0
Çine	222/b	623	610	624	585	8.2
Average values (°C, kbar)		628	611	629	611	7.3

but not with albite in the eclogites, this equilibrium gives minimum pressures. The fresh eclogites from the Kiraz area, which contain omphacite with Jd contents varying between 40 and 52 mol.%, indicate an average minimum pressure of 15 kbar at 630 °C (Fig. 11; Table 5). Similarly, maximum Jd contents of 47 mol.% in omphacites from the Alaşehir eclogites yield a minimum pressure of 15 kbar at 630 °C. The same barometer was also applied to the eclogitic metagabbros that reached the most advanced stages of transformation. The geobarometer indicates pressures of 12 kbar at 630 °C (Table 5).

The pressures in the garnet–amphibolites are estimated using the garnet+hornblende+plagioclase+quartz geobarometer of Kohn and Spear (1989). The calculated pressures vary from 4.9 to 9.5 kbar with an average value of approximately 7.3 kbar at 625 °C (Table 6). These pressure values are consistent with results from the Raase (1974) diagram based on the Al^{VI} vs Si contents of hornblende (Fig. 13).

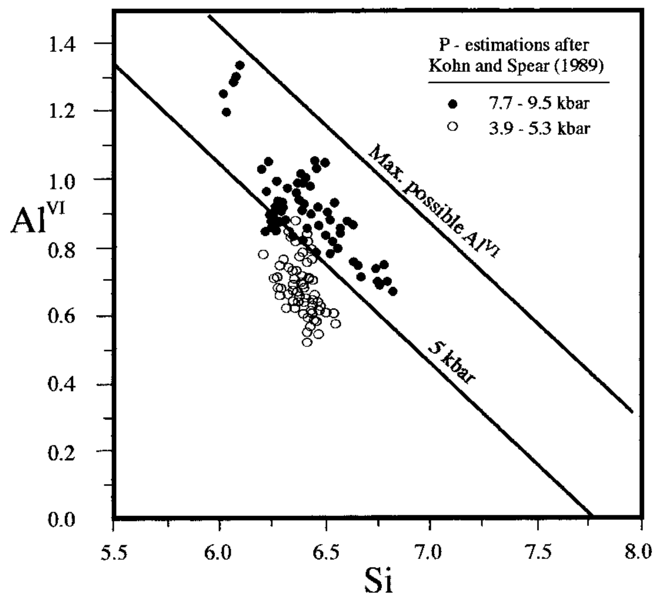

Fig. 13 Amphiboles from garnet amphibolites plotted on Al^{VI} vs Si diagram. (After Raase 1974)

Discussion and conclusion

The Pan-African basement of the Menderes Massif is made up of Late Proterozoic supracrustal metasediments, i.e., paragneisses and metapelites, which were intruded by numerous post-metamorphic (Dora et al. 1995) Pan-African (meta)granites, dated at approximately 550 Ma using the single zircon method (Hetzel and Reischmann 1996). Furthermore, the Pan-African basement also includes widespread basic igneous rocks, metagabbros, and metanorites as stocks and vein rocks. The restriction of the metagabbros to the Pan-African basement indicates that these rocks intruded the basement series before the deposition (or tectonic juxtaposition?) of the Paleozoic sequence. Furthermore, the recognition of the gabbros as partially assimilated xenoliths in the Pan-African metagranites clearly indicates the Precambrian age of the metagabbros.

In recent years relic phases and assemblages related to the Pan-African metamorphic evolution at granulite-, eclogite-, and amphibolite-facies conditions have commonly been detected in the Pan-African basement of the Menderes Massif (Candan and Dora 1998). Metamorphic monazites from granulite-facies orthopyroxene augen gneisses from the Birgi area yielded a Pan-African age of 660+61/–63 Ma (Warkus et al. 1998). Although preliminary results from zircons from the eclogites favor a Pan-African age (K. Mezger; pers. commun., in Warkus et al. 1998), there is no direct data for the age of the eclogite-facies metamorphism in the basement of the Menderes Massif. The amphibolite facies metamorphism in the Pan-African basement, which was characterized by widespread migmatization and palingenetic granite generation, caused common retrograde transformations of the former high-pressure and high-temperature mineral assemblages. This late phase of Pan-African metamorphism was dated at approximately 551 and 540 Ma by Hetzel et al. (1998) and Dannat and Reischmann (1998), respectively. On the other hand, the Pan-African metagranites/orthogneisses, which include the migmatites as xenoliths reaching up to several hundred of meters in diameter, have not experienced the high-pressure and high-temperature events and postdate the Pan-African metamorphism (Candan and Dora 1998). Similarly, the metabasic rocks in the Paleozoic metasediments of the cover series lack the high-pressure phases and do not display any textural evidence of decompression. This indirect geological evidence suggests a Pan-African age for the eclogites in the basement units.

The country rocks in the Pan-African basement of the Menderes Massif almost completely lack direct evidence for high-pressure metamorphism; however, in one locality in the Alasehir area (Fig. 3), gneisses which include eclogite lenses and layers contain Na-rich clinopyroxene relics and clinopyroxene+plagioclase symplectitic intergrowths. Furthermore, the great majority of eclogitic metagabbros occur as stocks and sill-like bodies in the paragneisses and schists, which represent a regular succession of metapsammitic to metapelitic rocks (Dora et al. 1998). This evidence suggests that the eclogitization of the metagabbros occurred in-situ and the high-pressure metamorphic event affected the whole basement of the Menderes Massif, with the notable exception of the orthogneisses, during the Pan-African orogeny.

The effects of the Pan-African orogeny are recognized in the Bitlis, Kırşehir, and Menderes crystalline complexes in Anatolia (Şengör et al. 1984; Okay et al. 1985; Dora et al. 1995). Intense Alpine deformation has resulted in internal imbrication of these crystalline complexes and obscured the evidence related to the Pan-African evolution (Okay et al. 1985; Partzsch et al. 1998; Gessner et al. 1998). Evidence for high-pressure metamorphism of probable Pan-African age was first described in the Bitlis Massif by Okay et al. (1985). Kyanite-eclogites, which occur in high-grade gneisses and micaschists, are believed to have been caused by thickening of the continental crust by overthrusting during the Pan-African orogeny. The eclogites in the Menderes Massif, which are similar in terms of geological setting and mineral composition to some "medium-temperature" (Carswell 1990) or "Group-B" (Coleman et al. 1965) eclogites, can be correlated to the Bitlis eclogites and are of considerable tectonic significance in revealing the common Pan-African high-pressure evolution of these two crystalline complexes. A possible tectonic model, similar to that of Bitlis Massif, is envisaged for the Menderes Massif, wherein the eclogite occurrences are related to the extreme crustal thickening induced by continental collision (Cuthbert et al. 1983; Indares 1993; Wilkerson et al. 1988).

Petrographic and chemical evidence reveals the existence of pre-, syn-, and post-eclogite mineral assemblages in the eclogites and eclogitic metagabbros. The high-pressure evolution of the Pan-African basement can be outlined as follows:

1. Pre-eclogitic stage. This stage is mainly represented by amphibolite-facies inclusions in garnets.
2. Syn-eclogitic stage. The basic igneous rocks and possibly their country rocks were buried to a depth of approximately 50 km and underwent high-pressure metamorphism at a minimum pressure of approximately 15 kbar and at a temperature of 644 °C.
3. Post-eclogitic stage. Post-eclogite, amphibolite-facies metamorphism at approximately 7 kbar and 623 °C indicates that the post-eclogitic uplift occurred under conditions of isothermal decompression.

The relation of the granulite-facies metamorphism indicated by the orthopyroxene relics in the gneisses and charnockites (Oberhänsli et al. 1997; Candan and Dora 1998) to the high-pressure event is still controversial. There is no direct evidence for any temperature increase during the post-eclogitic stage (Fig. 11); thus, the granulite facies metamorphism probably occurred during an early stage of the Pan-African evolution of the Precambrian basement of the Menderes Massif.

Acknowledgements This work was supported by TÜBITAK projects YDABCAG nos. 494 and 554, DFG-Project OB80/12 and by the Volkswagen-Stiftung. We thank T. Reischmann of Johannes Gutenberg Universität-Mainz for the use of the microprobe facilities. A. Okay and L. Franz are thanked for their thorough review which greatly improved the manuscript. The authors also greatfully acknowledge S. Mittwede and O. Kaya for editing the English.

References

Baker AJ (1986) Eclogitic amphibolites from the Grampian Moines. Min Mag 50:217–221

Bhattacharya A, Mohanty L, Maji A, Sen SK, Raith M (1992) Non-ideal mixing in the phlogopite–allinite binary: contrasts from experimental data on Mg–Fe partitioning and a formulation of the biotite–garnet geothermometer. Contrib Mineral Petrol 111:87–93

Candan O (1994) Petrography and metamorphism of the metagabbros at the northern part of Alasehir; Demirci-Gördes submassif of the Menderes Massif. Geol Bull Turkey 37:29–40 (in Turkish with English summary)

Candan O (1996) Petrography and metamorphism of the gabbros around Kiraz-Birgi region, Ödemis-Kiraz submassif of the Menderes Massif. Yerbilimleri 18:1–25 (in Turkish with English summary)

Candan O, Dora OÖ (1998) Granulite, eclogite and blueschists relics in the Menderes Massif: an approach to Pan-African and Tertiary metamorphic evolution. Geol Bull Turkey 41:1–35 (in Turkish with English summary)

Candan O, Dora OÖ, Dürr S, Oberhänsli R (1994) Erster Nachweis von Granulit-und Eklogit-Relikten im Menderes Massiv/Türkei. Göttingen. Abr Geol Paläontol 5:217–220

Candan O, Dora OÖ, Oberhänsli R, Oelsner FC, Dürr S (1997) Blueschist relics in the Mesozoic series of the Menderes Massif and correlation with Samos Island, Cyclades. Schweiz Mineral Petrol Mitt 77:95–99

Candan O, Dora OÖ, Oberhänsli R, Çetinkaplan M, Partzsch JH, Dürr S (1998) Pan-African high-pressure metamorphism in the Precambrian basement of the Menderes Massif, Western Anatolia, Turkey. Abstract 3th Int Turkish Geol Symp, p 275

Carswell AD (1990) Eclogite facies rocks. Blackie, London

Coleman RG, Lee DE, Beatty LB, Brannock WW (1965) Eclogites and eclogites: their differences and similarities. Geol Soc Am Bull 76:483–508

Cuthbert SJ, Harvey MA, Carswell DA (1983) A tectonic model for the metamorphic evolution of the Basal Gneiss Complex, Western South Norway. J Metam Geol 1:63–90

Çetinkaplan M (1995) Geochemical, mineralogical and petrographical investigation of the eclogites in southern part of Tire area, Ödemis-Kiraz Submassif of Menderes Massif. Master's thesis, D.E.Ü. Graduate School of Nature and Applied Sciences, Izmir, Turkey, 92 pp

Dannat C, Reischmann T (1998) Single zircon ages of migmatites from the Menderes Massif, SW Turkey. Programm des Workshops "Das Menderes Massiv (Türkei) und seine Nachbargebiete", 30 November to 1 December 1998 Mainz, 6 (Abstr)

De Wit MR, Strong F (1975) Eclogite bearing amphibolites from the Appalachian mobile belt, northwest Newfoundland: dry vs wet metamorphism. J Geol 83:609–627

Dora OÖ, Savaşçin Y, Kun N, Candan O (1987) Postmetamorphic plutons in the Menderes Massif. Yerbilimleri 14:79–89 (in Turkish with English summary)

Dora OÖ, Candan O, Dürr S, Oberhänsli R (1995) New evidence concerning the geotectonic evolution of the Menderes Massiv. Proc Int Earth Sci Colloq on the Aegean Region, 1995, Izmir, Turkey 1:53–72

Dora OÖ, Candan O, Kaya O, Koralay OE, Dürr S (1998) Revision of the leptites in the Menderes Massif: a supracrustal metasedimentary origin. Abstract 3rd Int Turkish Geol Symp, Ankara, Turkey, p 283

Dürr S (1975) Über Alter und geotektonische Stellung des Menderes Kristallins/SW-Anatolien und seine Äquivalente in der Mittleren Aegean. Habilitation thesis, Univ Marburg, pp 1–107

Dürr S, Altherr R, Keller J, Okrusch M, Seidel E (1978) The median Aegean crystalline belt: stratigraphy, structure, metamorphism, magmatism. In: Closs H, Poeder DH, Schmidt K (eds) Alps, Apennines, Hellenides. Schweizerbart, Stuttgart, pp 455–477

Ellis DJ, Green DH (1979) An experimental study of the effects of Ca upon garnet–clinopyroxene Fe–Mg exchange equilibria. Contrib Mineral Petrol 71:13–22

Essene EJ, Fyfe WS (1967) Omphacite in Californian metamorphic rocks. Contrib Mineral Petrol 15:1–23

Ferry JM, Spear FS (1978) Experimental calibration of the partitioning of Fe and Mg between biotite and garnet. Contrib Mineral Petrol 66:113–117

Gessner K, Ring U, Lackmann W, Passchier CW, Güngör T (1998) Structure and crustal thickening of the Menderes Massif, Southwest Turkey, and consequences for large-scale correlations between Greece and Turkey. Bull Geol Soc Greece 32:145–152

Graham CM, Powell R (1984) A garnet–hornblende geothermometer: calibration, testing and application to the Pelona schist, southern California. J Metam Geol 2:13–31

Griffen WL, Heier KS (1973) Petrological implications of some corona structures. Lithos 6:315–335

Hetzel R, Reischmann T (1996) Intrusion age of Pan-African augen gneisses in the southern Menderes Massif and the age of cooling after Alpine ductile extensional deformation. Geol Mag 133:565–572

Hetzel R, Romer RL, Candan O, Passchier CW (1998) Geology of the Bozdag area, central Menderes Massiv, SW Turkey: Pan-African basement and Alpine trusting. Geol Rundsch 87:394–406

Holland TJB (1980) The reaction albite=jadeite+quartz determined experimentally in the range 600–1200 °C. Am Mineral 65:129–134

Indares A (1993) Eclogitized gabbros from the eastern Grenville provence: textures, metamorphic context and implications. Can J Earth Sci 30:159–173

Kohn MJ, Spear FS (1989) Empirical calibration of geobarometers for the assemblage garnet+hornblende+plagioclase+quartz. Am Mineral 74:77–84

Krogh EJ (1982) Metamorphic evolution of Norwegian country-rock eclogites, as deduced from mineral inclusions and compositional zoning in garnets. Lithos 15:305–321

Krogh EJ (1988) The garnet–clinopyroxene Fe–Mg geothermometer: a reinterpretation of existing experimental data. Contrib Mineral Petrol 99:44–48

Laird J, Albee AL (1981) Pressure, temperature and time indicators in mafic schists: their application to reconstructing the polymetamorphic history of Vermont. Am J Sci 281:127–175

Leake BA, Woolley AR, Arps CES, Birch WD, Gilbert MC, Grice JD, Hawthorne FC, Kato A, Kisch HJ, Krivovichev VG, Linthout K, Laird J, Mandarino J, Maresch WV, Nickel EH, Rock NMS, Schumacher JC, Smith DC, Stephonson NCN, Ungaretti L, Whittaker EJW, Youzmi G (1997) Nomenclature of amphiboles. Report of the subcommittee on amphiboles of the international mineralogical association commission on new minerals and mineral names. Eur J Mineral 9:623–651

Mork MBE (1985) A gabbro to eclogite transition on Flemsoy, Sunnmore, western Norway. Chem Geol 50:283–310

Oberhänsli R, Candan O, Mezger K, Dora OÖ, Dürr S (1995) Eclogites and granulites in the Menderes Massif, western Turkey. Terra Abstr 8:18

Oberhänsli R, Candan O, Dora OÖ, Dürr S (1997) Eclogites within the Menderes Crystalline Complex/western Turkey/Anatolia. Lithos 41:135–150

Oberhänsli R, Monie P, Candan O, Warkus FC, Partzsch JH, Dora OÖ (1998) The age of blueschist metamorphism in the Mesozoic cover series of the Menderes Massif. Schweiz Mineral Petrogr Mitt 78:309–316

Okay AI, Arman MB, Göncüoğlu MC (1985) Petrology and phase relations of the kyanite eclogites from eastern Turkey. Contrib Mineral Petrol 91:196–204

Önay TS (1949) Über die Smirgelgesteine SW-Anatoliens. Schweiz Mineral Petrol Mitt 29:359–484

Partzsch JH, Oberhänsli R, Candan O, Warkus FC (1998) The evolution of the central Menderes Massif, West Turkey: a complex nappe pile recording 1.0 Ga of geological history. Freiberger Forschungsheft C-471:166–168

Perchuk LL, Lavrent'eva IV (1983) Experimental investigation of exchange equilibria in the system cordierite–garnet–biotite. In: Saxena SK (ed) Kinetics and equilibrium in mineral reactions. Advances in physical geochemistry, vol 3. Springer, Berlin Heidelberg New York, pp 199–239

Raase P (1974) Al and Ti contents of hornblende, indicators of pressure and temperature of regional metamorphism. Contrib Mineral Petrol 45:231–236

Rahn M (1991) Eclogites from the Minugrat, Siviez-Mischabel nappe (Valais, Switzerland). Schweiz Mineral Petrogr Mitt 71:415–426

Rivers T, Mengel FC (1988) Contrasting assemblages and petrogenetic evolution of corona and noncorona gabbros in the Grenvince Province of western Labrador. Can J Earth Sci 25:1629–1648

Şengör AMC, Satır M, Akkök R (1984) Timing of tectonic events in the Menderes Massif, western Turkey. Implications for tectonic evolution and evidence for Pan-African basement in Turkey. Tectonics 3:693–707

Warkus FC, Partzsch JH, Candan O, Oberhänsli R (1998) The tectono-metamorphic evolution of the Birgi-Tire nappe in the Menderes massif, SW-Turkey. Freiberger Forschungsheft C-471:237–238

Wilkerson A, Carlson WD, Smith D (1988) High-pressure metamorphism during the Llano orogeny inferred from Proterozoic eclogite remnants. Geology 16:391–394